Ion hydration and associated defects in hydrogen bond network of water: Observation of reorientationally slow water molecules beyond first hydration shell in aqueous solutions of $MgCl_2$

Upayan Baul* and Satyavani Vemparala†
The Institute of Mathematical Sciences, C.I.T. Campus, Taramani, Chennai 600113, India
(Received 3 April 2014; revised manuscript received 25 November 2014; published 8 January 2015)

Effects of the presence of ions, at moderate to high concentrations, on dynamical properties of water molecules are investigated through classical molecular dynamics simulations using two well-known nonpolarizable water models. Simulations reveal that the presence of magnesium chloride ($MgCl_2$) induces perturbations in the hydrogen bond network of water leading to the formation of bulklike domains with "defect sites" on boundaries of such domains: water molecules at such defect sites have less number of hydrogen bonds than those in bulk water. Reorientational autocorrelation functions for dipole vectors of such defect water molecules are computed at different concentrations of ions and compared with system of pure water. Earlier experimental and simulation studies indicate significant differences in reorientational dynamics for water molecules in the first hydration shell of many dissolved ions. Results of this study suggest that defect water molecules, which are beyond the first hydration shells of ions, also experience significant slowing of reorientation times as a function of concentration in the case of $MgCl_2$. However, addition of cesium chloride (CsCl) to water does not perturb the hydrogen bond network of water significantly even at higher concentrations. This difference in behavior between $MgCl_2$ and CsCl is consistent with the well-known Hofmeister series.

DOI: 10.1103/PhysRevE.91.012114 PACS number(s): 61.20.−p, 82.30.Rs, 83.10.Mj

I. INTRODUCTION

Effects of simple inorganic salts on the molecular properties of water are at the heart of a vast number of interesting and complex processes such as the stability of proteins and nucleic acids [1] and environmentally relevant processes [2,3]. Understanding the effect of dissolved ions on the structural and dynamical properties of water is essential in this regard. The Hofmeister effect, which includes highly ion-specific effects on aggregation dynamics of proteins [4,5] and other biologically relevant processes [5–7], has been of significant interest lately. Spectroscopic techniques have been instrumental in probing the cooperative ion hydration mechanism and consequent long-range structural and dynamical effects of certain salts, or ion combinations, on water [8–14]. Earlier experiments suggested that the effect of ions on dynamical properties of water is largely restricted to their first hydration shell [15,16]. However, recent experiments, using a combination of femtosecond time-resolved infrared (fs-IR) and dielectric relaxation spectroscopy, have shown the existence of a fraction of reorientationally slow water molecules [8,9] well beyond the first hydration shells of dissolved $MgSO_4$ ions. In these experiments, two subpopulations of water molecules were identified for various salts: one with reorientation time scales comparable to pure water (∼2.6 ps) and the other showing characteristically slower reorientations (∼10 ps). The fraction of total water molecules contributing to the subpopulation of slow-water molecules was seen to increase with increase in salt concentration for all salts, and the magnitude of increase was observed to be highly dependent on ion combinations: being largest for combinations of strongly hydrated ion species (Mg^{2+}, SO_4^{2-}).

Despite the recent experimental results [8], the existence of long-range temporal effects of salts, beyond the first hydration shell, is controversial owing to results from other experimental [15–18] as well as simulation [17,19–22] studies which suggest the contrary. While an intense cooperative slowdown of water reorientation has been observed in the presence of ions with high charge densities, the range of presence of slow water molecules has been found to be confined to the first hydration shell of the ions [16,17,19–22]. The focus of present work is on the extended hydrogen bond network in bulk water and the domain formation and existence of "defect water molecules" at boundaries of such domains when salt is added. Instead of classifying water molecules based on radially varying spherical hydration shells around ions, subpopulations depending on whether they are bulklike or defect water molecules are considered. Using molecular dynamics (MD) simulations, we present evidence for reorientational slowing of water molecules well beyond the first hydration shell for solutions of $MgCl_2$ and the effect of salt concentration on the same. However, for CsCl-water solutions, no significant effect on reorientational dynamics of water (irrespective of CsCl concentration) was found, which is in good agreement with the Hofmeister series.

II. METHODS

A. System setup

Classical atomistic molecular dynamics (MD) simulations were performed with TIP4P-Ew [23] and TIP3P [24] water models and using simulation package NAMD 2.9 [25]. For simulations involving TIP4P-Ew water model, recently developed parameters for divalent ion Mg^{2+} and optimized for correct coordination number [26] were used. Monovalent (Cl^-, Cs^+) ion parameters for the TIP4P-Ew simulations were taken from extensively used halide and alkali ion parameters [27]. Standard CHARMM parameters were used for all ions [28] while simulating with TIP3P water. All systems were first equilibrated under constant pressure and temperature (NPT) and further under constant volume and

*upayanb@imsc.res.in
†vani@imsc.res.in

 ©2015 American Physical Society

energy (NVE) conditions. Production runs for all systems were performed under NVE conditions. For the NPT simulations, pressure was maintained at 1 atm using Langevin Piston [29], and temperature coupling to an external heat bath was used to maintain temperature at 298 K for simulations with TIP4P-Ew model and at 305 K for TIP3P. Lennard-Jones interactions were smoothly truncated with cutoff 12 Åusing a switching function between 10 Å and 12 Å. Long-range electrostatic interactions were computed using particle mesh Ewald (PME) method. Time steps of 1 and 2 fs were used for simulations involving TIP4P-Ew and TIP3P models, respectively.

TIP4P-Ew water systems. Initially a 54 Å × 54 Å × 54 Å box of water containing 5251 water molecules was equilibrated for 5 ns under NPT conditions and further for 4 ns under NVE. *Solvate* plugin of VMD [30] was used to produce $MgCl_2$ (2 M, 3 M, 4 M) and CsCl (3 M, 4 M) solutions from this equilibrated configuration, and each of the salt-water systems was equilibrated for 5 ns under NPT conditions and a further 4 ns under NVE resulting in a total equilibration time of 9 ns for each of six systems involving TIP4P-Ew water.

TIP3P water systems. Initially a 50 Å × 50 Å × 50 Å box of water containing 4972 water molecules was equilibrated for 10 ns under NPT conditions. *Solvate* plugin of VMD was used to produce salt solutions of the same concentrations as for TIP4P-Ew water molecules from this equilibrated configuration, and each of these salt-water systems was equilibrated for 15 ns under NPT conditions. The pure water system was further simulated for 5 ns, resulting in 15 ns NPT equilibration simulations for each of the six systems considered. All the above systems were equilibrated for a further 9 ns under NVE conditions resulting in total equilibration time of 24 ns for systems involving TIP3P water.

Further details of system setup are included in Table SI [31]. Relatively high salt concentrations of salt were chosen in this study based on recently studied experimental concentrations [9,18] as well as to account for good statistics. For computation of reorientational autocorrelation functions and other dynamic observables, production runs of 1 ns each were carried out for all systems under NVE conditions, with system configurations saved every 0.1 ps. All the dynamical analyses were performed over the last 0.5 ns of the production run data.

B. Water domain identification

To identify hydrogen bond (O-O distance $\leqslant$ 3.8 Å and H-O··H angle $\leqslant 60^\circ$ definition of hydrogen bond was used in the present study) network domains in all 12 systems considered in this study, each system was divided into multiple overlapping slabs along each of the three orthonormal directions. Over each such slab, hydrogen bonded domains of water molecules were identified. The criterion for inclusion of water molecules to a single domain is the existence of a bidirected path between every pair, via a network of hydrogen bonds formed by water molecules in the same slab. Using this definition of water domain, it was observed that for pure water all values of slab thickness $\geqslant$2.7 Å consistently resulted in a single spanning domain along the slab. Addition of salt to the water systems resulted in formation of multiple water domains, even when higher values of slab thickness (4 Å) were considered. The size distribution of different domains of

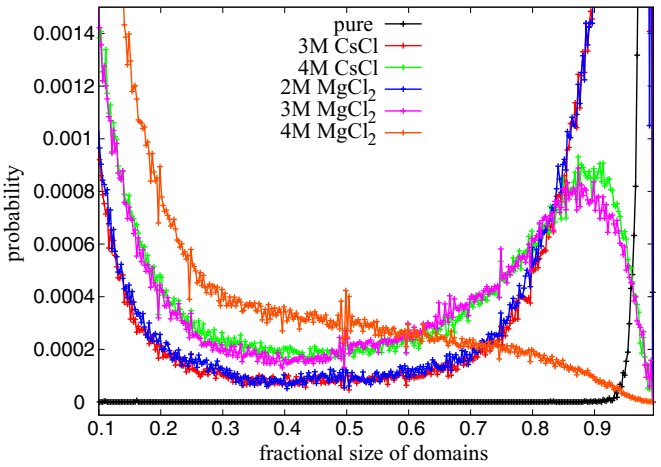

FIG. 1. (Color online) Domain size distribution plots scaled to [0,1] for all systems with TIP4P-Ew water model considered in the study and for slab thickness of 4 Å. The data are averaged over 5000 frames and 0.5 ns of simulation time. In the left side of the figure, plots moving from down to up are for pure water, followed by 3 M CsCl and 2 M $MgCl_2$ (overlapping), followed by 3 M $MgCl_2$ and 4 M CsCl (overlapping) and finally 4 M $MgCl_2$.

TIP4P-Ew water systems for a slab thickness of (4 Å) and various concentrations of added salts, in comparison with the case of pure water, is shown in Fig. 1. From the figure, it can be seen that for the case of pure water, a single spanning domain exists. With the addition of $MgCl_2$ salt, the size distribution of water domains depends on the concentration. For 2 M salt concentration, the domain size distribution is similar to the pure water case, with the additional appearance of smaller water domains. When the concentration of $MgCl_2$ is increased to 3 M and above, the domain size distribution differs significantly from that of pure water. No single spanning domain remains in the system, and the system primarily consists of many domains of water molecules of varying size distribution. Similar behavior is also observed when the TIP3P water model is used, and the results are given in Fig. SI [31]. Ion-specific local structural effects on water have been widely studied in the literature [16,32–36], generally classifying ions into structure makers and structure breakers [6,36–38] based on their effect on the hydrogen bond network of water. High charge density ions have been known to exert strong patterning effects on first solvation shell water molecules leading to a reduction in water-water hydrogen bonding [39–41].

The domain size distribution in a CsCl-water system, in contrast to $MgCl_2$-water systems, is very similar to the pure water system even at 4 M concentration consistent with a recent *ab initio* MD study of other low-charge density salts such as NaCl and CsI [42]. Following the identification of domains, water molecules residing at the domain boundaries were identified and recorded for all three orthonormal directions. From these data, the water molecules which appear in all three lists, corresponding to three orthonormal directions, are identified and labeled defect water molecules. This set of defect water molecules, however, may contain water molecules which are within the first hydration shell of any ions. From this superset of defect water molecules, a subset of water molecules which are not within the first hydration shell of any ion were

identified, which are referred to henceforth as *waterD* (pure water is referred to as *waterP*). A further subpopulation of defect water molecules were also identified: water molecules which are at domain boundaries in any two orthonormal directions (instead of three) and not in the first hydration shell of ions. These will be referred to as *waterD2* and constitute a more relaxed definition of defect water molecules, and their subpopulation size would be larger than that of *waterD* at moderate salt concentrations.

The probability distribution of local tetrahedral order parameter (Q) was computed for *waterP* and subpopulations *waterD* for systems involving the TIP4P-Ew model of water. Q for a water molecule is defined as [43]

$$Q = 1 - \frac{3}{8}\sum_{j=1}^{3}\sum_{k=j+1}^{4}\left(\cos\Psi_{jk} + \frac{1}{3}\right)^2 \quad (1)$$

where Ψ_{jk} is the angle formed by the lines joining the oxygen atom of a given molecule and those of its nearest neighbors j and k ($\leqslant 4$). Q takes values 1 and 0 for ideal tetrahedral structures and ideal gas, respectively.

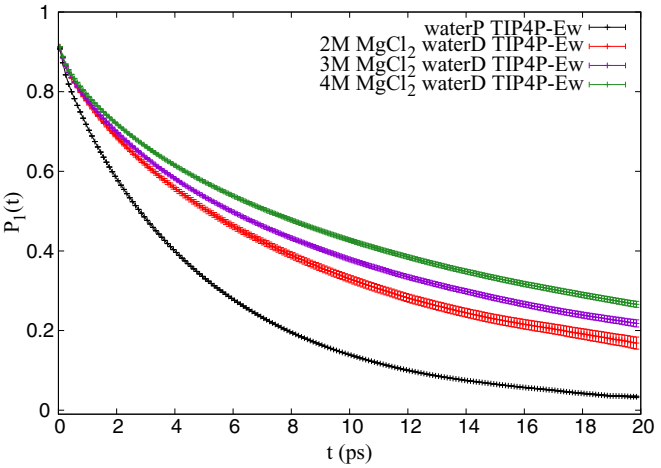

FIG. 2. (Color online) Plots for $P_1(t)$ for *waterD* in the presence of $MgCl_2$ (colored curves) at the concentrations studied and pure water (black) using TIP4P-Ew model. The error bars in all plots have been magnified five times. Plots moving from down to up are for *waterP*, followed by *waterD* for 2 M, 3 M, and 4 M $MgCl_2$.

III. RESULTS

The tetrahedrality results, in conjunction with hydrogen bonds per water molecules, suggest that the subpopulation of *waterD* molecules differ significantly from pure water molecules. The typical bimodal distributions [43,44] of tetrahedrality of water molecules, measured as in Eq. (1), exhibit deviations in the case of defect water molecules (results are included in Fig. SV [31]). The number of hydrogen bonds per defect water molecule (*waterD*) was found to be less than 2. Reorientation autocorrelation functions $P_1(t)$ and $P_2(t)$ defined as first and second Legendre polynomials of water dipole vector ($\vec{p}$), a unit bisector of the H-O-H angle, were computed for various subpopulations of water molecules over 20 ps:

$$P_1(t) = \langle \overrightarrow{p(t)}.\overrightarrow{p(0)} \rangle, \quad (2)$$

$$P_2(t) = \left\langle \tfrac{1}{2}\{3\cos^2[\overrightarrow{p(t)}.\overrightarrow{p(0)}] - 1\} \right\rangle \quad (3)$$

where the angular brackets denote average over the number of water molecules in each subpopulation and time. The errors for $P_1(t)$ and $P_2(t)$ have been obtained by computing standard deviations using block averages.

The computed correlation functions $P_1(t)$ for pure water and $MgCl_2$ solutions using TIP4P-Ew water model are plotted in Fig. 2 [plots of $P_2(t)$ for TIP4P-Ew and both $P_1(t)$ and $P_2(t)$ for TIP3P are given in Fig. SII and Fig. SIII, respectively [31]]. A significant slowing of reorientational times for subpopulation *waterD* as a function of salt concentration can be seen in the figure. These results suggest that "slow water molecules" exist beyond the first hydration shell of both cations and anions. Earlier experiments and simulations show that the propensity of formation of ion-water clusters is higher at higher concentration of salts in water [45]. Water molecules trapped in such clusters can experience very slow reorientational times. It is to be noted that though the salt concentrations considered in this study are high, the sampling of subpopulation *waterD* will not include such trapped water molecules, by definition. The *waterD* molecules considered can, at best, be part of three solvent-separated ion pairs. Extensive studies of the reorientation of water molecules [46–50] have shown that autocorrelation functions of a body-set vector, including dipole vector, of water molecules involve distinct time scales. A fast, subpicosecond decay due to librational motion is followed by a slower component that can be attributed to structural changes such as hydrogen bond exchange and reorientations of hydrogen-bonded water molecules. Multiexponential functions thus serve as good fit functions for such correlations, and they have been fit to either bi- ($A_3 = 0$) or triexponential functions of the form $P_{1/2}(t) = A_1\exp(-\frac{t}{\tau_1}) + A_2\exp(-\frac{t}{\tau_2}) + A_3\exp(-\frac{t}{\tau_3})$ depending on the system. However, the attribution of specific physical processes to these time constants is not attempted in this work. A biexponential function ($A_3 = 0$) was the best fit for reorientational time curves for the pure water case. In the presence of $MgCl_2$, a triexponential function was found to be more appropriate, with dynamics of defect water molecules introducing a new time scale into the problem. The decay times (τ_3) are much larger than the slowest component of orientational relaxation for bulk water and show an increase with the concentration of $MgCl_2$ salt. These results are shown in Table I. Simulation results show that for the largest concentration of $MgCl_2$ studied (4 M), the longest mode in decay time for defect water molecules, which are beyond first hydration shell of any ions, is as high as 21 ps. The $P_1(t)$ curves for CsCl salt solutions are plotted in Fig. 3, and deviation from the case of pure water is much less significant compared to effects of $MgCl_2$ and independent of salt concentration. The $P_1(t)$ curves for CsCl are also fit with a triexponential function, and the values are given in Table I. The corresponding reorientational time constants obtained for $P_2(t)$ for subpopulation *waterD* for TIP4P-Ew and $P_{1/2}(t)$ for TIP3P water models are given in Table SII [31]. The anion used in both the salts, Cl^-, is known to be weakly hydrated ion, and such anions are expected to affect the dynamics of OH vector preferentially over dipole vector of a water molecule [9]. Thus the observed difference in reorientational

TABLE I. Water reorientational time constants [for $P_1(t)$] with TIP4P-Ew water model [under NVE conditions following NPT ($T = 298$ K) simulations] for pure water molecules and *waterD* subpopulation in the presence of salt using triexponential fits. All time constants are in picoseconds.

Salt	Subpopulation	A_1	τ_1	A_2	τ_2	A_3	τ_3
None		0.078(±0.002)	0.329(±0.052)	0.848(±0.002)	5.333(±0.034)		
$MgCl_2$	(2M,*waterD*)	0.052(±0.004)	0.209(±0.058)	0.262(±0.003)	3.538(±0.031)	0.615(±0.002)	15.027(±0.002)
	(3M,*waterD*)	0.049(±0.003)	0.192(±0.028)	0.222(±0.003)	3.010(±0.016)	0.656(±0.003)	17.654(±0.001)
	(4M,*waterD*)	0.050(±0.002)	0.206(±0.024)	0.197(±0.002)	2.980(±0.017)	0.682(±0.002)	20.818(±0.001)
CsCl	(3M,*waterD*)	0.044(±0.004)	0.188(±0.307)	0.169(±0.005)	1.917(±0.039)	0.720(±0.003)	7.476(±0.002)
	(4M,*waterD*)	0.052(±0.003)	0.232(±0.031)	0.235(±0.009)	2.788(±0.022)	0.644(±0.002)	8.506(±0.002)

dynamics between the two cations studied in this work, Mg^{2+} and Cs^+, reflects the difference between a strongly hydrated versus a weakly hydrated cation, while both have the same counterion. Similar differences between Mg^{2+} and Cs^+ are observed for the subpopulation of water molecules *waterD2* as well, and the results are included in Fig. SIV [31] for both water models used. These results seem to be consistent with the ordering of cations in the well-known Hofmeister series [9].

Two dynamical quantities, which can be measured experimentally, related to ion hydration are the hydration number ($N_{\vec{p}}$), defined as the number of moles of slow water dipoles per mole of dissolved salt, and fraction of slow water molecules relative to bulklike water ($f_{\frac{\text{slow}}{\text{bulk}}}$) [8,9]. The slow water molecules identified in the experiments are independent of structural definition of hydration shells and can contain water molecules within and outside the first hydration shells of ions. To be consistent with the experiments, a similar definition of slow water molecules was adopted which entails including water molecules in the first hydration shell of cations along with two subpopulations *waterD* and *waterD2*. Further, simulations allow a new dynamical quantity $f_{(\frac{\text{slow}}{\text{bulk}},\text{defect})}$ to be computed, which is difficult to measure experimentally. $f_{(\frac{\text{slow}}{\text{bulk}},\text{defect})}$ measures the fraction of slow water molecules beyond the first hydration shell of ions relative to bulklike water. The $N_{\vec{p}}$, $f_{\frac{\text{slow}}{\text{bulk}}}$, and $f_{(\frac{\text{slow}}{\text{bulk}},\text{defect})}$ for both $MgCl_2$ and CsCl solutions are given in Table II. The corresponding numbers for the TIP3P water model are given in Table SIII [31]. It has been suggested that the typical hydration number, $N_{\vec{p}}$, for many ions is around 6, and any value greater than this number indicates presence of long-range effects of ions [8]. Experiments with salt solutions containing both strongly hydrated cations and anions show a large $N_{\vec{p}}$ value of the order of 18, and this has been suggested as a strong indication of cooperative slowing of water dynamics beyond first hydration shells of such ions [8]. In the present study the $N_{\vec{p}}$ values for $MgCl_2$ for all three concentrations studied is 7, indicating the existence of the long-range effect of Mg^{2+} ions in the presence of Cl^-, albeit weaker than when the counterion is SO_4^{2-}. The $N_{\vec{p}}$ values for CsCl were found to be less than 6.

From Table II, it can also be seen that the fraction of slow water molecules relative to bulklike water, beyond the first hydration shell ($f_{(\frac{\text{slow}}{\text{bulk}},\text{defect})}$), for 2 M $MgCl_2$ is only 0.06. This small value may suggest why long-range effects of strongly hydrated cations were not conclusively found in earlier simulations. A snapshot of $MgCl_2$-TIP4P-Ew water system for 2 M salt concentration is shown in Fig. 4. The defect water molecules, which are beyond the first hydration shell of any ions, are shown as van der Waals spheres, and it can be seen that they form a small fraction of the total number of water molecules in the system. Values of $f_{\frac{\text{slow}}{\text{bulk}}}$ as a function of radial distance from cations was computed and are given in Table SIV [31]. Within 2.5 Å, a typical radial distance defining the first hydration shell, the fraction of slow water molecules to bulk $f_{\frac{\text{slow}}{\text{bulk}}}$ for 2 M Mg Cl_2 concentration is 0.89. This value drops to 0.22 just above 3 Å and progressively decreases beyond the first hydration shell. However, the nonzero values

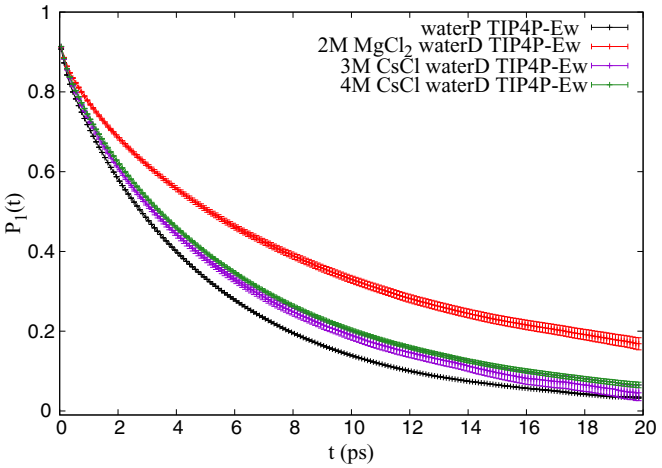

FIG. 3. (Color online) Plots for $P_1(t)$ for *waterD* comparing 3 M and 4 M CsCl with 2 M $MgCl_2$. The black curve is for pure water using TIP4P-Ew model. The error bars in all plots have been magnified five times. Plots moving from down to up are for *waterP*, followed by *waterD* for 3 M and 4 M CsCl (overlapping) and finally *waterD* for 2 M $MgCl_2$.

TABLE II. Approximate values of quantities $N_{\vec{p}}$, $f_{\frac{\text{slow}}{\text{bulk}}}$, and $f_{(\frac{\text{slow}}{\text{bulk}},\text{defect})}$ obtained with the TIP4P-Ew water model [under NVE conditions following NPT ($T = 298$ K) simulations]. The data are averaged over 5000 frames and 0.5 ns of simulation time.

Salt, conc.	$N_{\vec{p}}$	$f_{\frac{\text{slow}}{\text{bulk}}}$	$f_{(\frac{\text{slow}}{\text{bulk}},\text{defect})}$
$MgCl_2$, 2 M	7.28	0.19	0.06
$MgCl_2$, 3 M	7.05	0.41	0.26
$MgCl_2$, 4 M	6.71	0.80	0.34
CsCl, 3 M	5.91	0.05	0.03
CsCl, 4 M	5.80	0.15	0.10

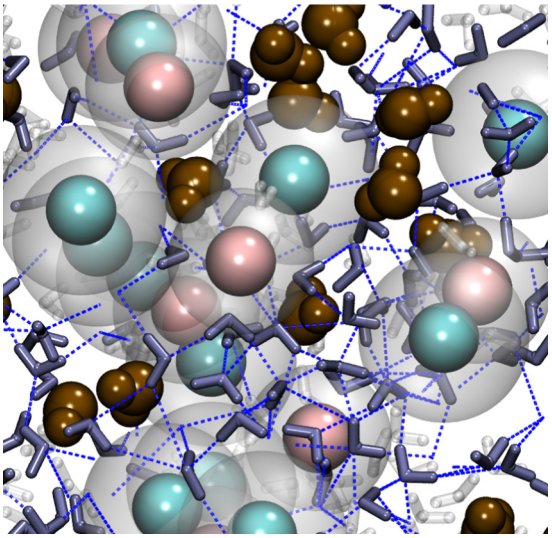

FIG. 4. (Color online) Snapshot of part of $MgCl_2$-water system at 2 M salt concentration. The Mg^{2+} and Cl^- ions are shown as cyan and pink spheres. The first hydration shells (2.5 Å radius) around the ions are also shown as transparent spheres. The defect water molecules, *waterD*, which are not within the first hydration shell, are shown in the vdW representation in brown, and the other water molecules are shown in a stick representation (transparent for water molecules in the first solvation shell of ions). The hydrogen bond network among water molecules is also shown.

of $f_{\frac{\text{slow}}{\text{bulk}}}$ well beyond the first and second hydrations shells of Mg^{2+} ions even at 2 M concentration indicate the delocalized presence of slow water molecules. Similar trends are observed for the TIP3P water model as well. These results suggest that classifying water molecules around multiple ions, at moderate to high concentrations, using an oft-used definition of radially varying hydration shells may not be able to capture this small fraction of slow water molecules. The definition of defect water molecules *waterD* used in this study can capture this small fraction of slow water molecules and can suggest long-range effects of strongly hydrated cations such as Mg^{2+}. It can also be seen from Table II that this fraction of defect water molecules increases with concentration, and a significant jump occurs in such a fraction from 2 M to 4 M (0.19 to 0.80). This suggests that a global network of defect water molecules may occur at higher salt concentrations. The values of $f_{\frac{\text{slow}}{\text{bulk}}}$ and $f_{(\frac{\text{slow}}{\text{bulk}},\text{defect})}$ for CsCl salt solutions are very small, consistent with results in Fig. 3.

IV. CONCLUSION

To summarize, MD simulation results in this study support the concentration-dependent effects of strongly hydrated ion species (Mg^{2+}) on the reorientational dynamics of water molecules beyond the first hydration shell. A likely mechanism for the same has been suggested in terms of salt induced defects in the underlying hydrogen bond network of water, which is in agreement with concepts of ion-induced patterning of water at long distances. While the actual number of water molecules beyond the first hydration shell of ions that exhibit slow reorientational times is a small fraction of the total water molecules, especially at low concentrations, they have been found at large spatial separations from the ions. The fractional number has been observed to increase monotonically with an increase in the concentration of $MgCl_2$. It is to be noted that the long-range effect of Mg^{2+} ions in the presence of a weakly hydrated counterion Cl^- is smaller than experimentally observed effects in the presence of SO_4^{2-} [8], but not insignificant. Comparison with a weakly hydrated cationic species (Cs^+) has been seen to be in agreement with the Hofmeister series. The results in the present study are obtained with two nonpolarizable models of water, and these results are expected to be enhanced when polarizable models of water are used and are a part of future studies.

ACKNOWLEDGMENT

All the simulations in this work have been carried out on 1024-cpu Annapurna cluster at The Institute of Mathematical Sciences, Chennai, India.

[1] P. L. Nostro and B. W. Ninham, Chem. Rev. **112**, 2286 (2012).
[2] R. J. Buszek, J. S. Francisco, and J. M. Anglada, Int. Rev. Phys. Chem. **30**, 335 (2011).
[3] P. Jungwirth and D. J. Tobias, Chem. Rev. **106**, 1259 (2006).
[4] F. Hofmeister, Arch. Exp. Pathol. Pharmakol. **24**, 247 (1888).
[5] W. Kunz, J. Henle, and B. W. Ninham, Curr. Opin. Coll. Int. Sci. **9**, 19 (2004).
[6] Y. Marcus, Chem. Rev. **109**, 1346 (2009).
[7] D. J. Tobias and J. C. Hemminger, Science **319**, 1197 (2008).
[8] K. J. Tielrooij, N. Garcia-Araez, M. Bonn, and H. J. Bakker, Science **328**, 1006 (2010).
[9] K. J. Tielrooij, S. T. van der Post, J. Hunger, M. Bonn, and H. J. Bakker, J. Phys. Chem. B **115**, 12638 (2011).
[10] J. T. OBrien, J. S. Prell, M. F. Bush, and E. R. Williams, J. Am. Chem. Soc. **132**, 8248 (2010).
[11] J. S. Prell, J. T. OBrien, and E. R. Williams, J. Am. Chem. Soc. **133**, 4810 (2011).
[12] J. T. OBrien and E. R. Williams, J. Am. Chem. Soc. **134**, 10228 (2012).
[13] S. T. v. d. Post and H. J. Bakker, Phys. Chem. Chem. Phys. **14**, 6280 (2012).
[14] D. Paschek and R. Ludwig, Angew. Chem. Int. Ed. **50**, 352 (2011).
[15] A. W. Omta, M. F. Kropman, S. Woutersen, and H. J. Bakker, J. Chem. Phys. **119**, 12457 (2003).
[16] A. W. Omta, M. F. Kropman, S. Woutersen, and H. J. Bakker, Science **301**, 347 (2003).
[17] S. Funkner, G. Niehues, D. A. Schmidt, M. Heyden, G. Schwaab, K. M. Callahan, D. J. Tobias, and M. Havenith, J. Am. Chem. Soc. **134**, 1030 (2011).

[18] C. H. Giammanco, D. B. Wong, and M. D. Fayer, J. Phys. Chem. B **116**, 13781 (2012).
[19] A. Vila Verde and R. Lipowsky, J. Phys. Chem. B **117**, 10556 (2013).
[20] G. Stirnemann, E. Wernersson, P. Jungwirth, and D. Laage, J. Am. Chem. Soc. **135**, 11824 (2013).
[21] L. Yang, Y. Fan, and Y. Q. Gao, J. Phys. Chem. B **115**, 12456 (2011).
[22] Y.-S. Lin, B. M. Auer, and J. L. Skinner, J. Chem. Phys. **131**, 144511 (2009).
[23] H. W. Horn, W. C. Swope, J. W. Pitera, J. D. Madura, T. J. Dick, G. L. Hura, and T. Head-Gordon, J. Chem. Phys. **120**, 9665 (2004).
[24] W. L. Jorgensen, J. Chandrasekhar, J. D. Madura, R. W. Impey, and M. L. Klein, J. Chem. Phys. **79**, 926 (1983).
[25] J. C. Phillips, R. Braun, W. Wang, J. Gumbart, E. Tajkhorshid, E. Villa, C. Chipot, R. D. Skeel, L. Kale, and K. Schulten, J. Comput. Chem. **26**, 1781 (2005).
[26] P. Li, B. P. Roberts, D. K. Chakravorty, and K. M. Merz, J. Chem. Theory Comput. **9**, 2733 (2013).
[27] I. S. Joung and T. E. Cheatham, J. Phys. Chem. B **112**, 9020 (2008).
[28] A. D. MacKerell *et al.*, J. Phys. Chem. B **102**, 3586 (1998).
[29] S. E. Feller, Y. Zhang, R. W. Pastor, and B. R. Brooks, J. Chem. Phys. **103**, 4613 (1995).
[30] W. Humphrey, A. Dalke, and K. Schulten, J. Mol. Graphics **14**, 33 (1996).
[31] See Supplemental Material at http://link.aps.org/supplemental/10.1103/PhysRevE.91.012114 for supplemental figures and tables.
[32] C. D. Cappa, J. D. Smith, B. M. Messer, R. C. Cohen, and R. J. Saykally, J. Phys. Chem. B **110**, 5301 (2006).
[33] L. A. Näslund, D. C. Edwards, P. Wernet, U. Bergmann, H. Ogasawara, L. G. M. Pettersson, S. Myneni, and A. Nilsson, J. Phys. Chem. A **109**, 5995 (2005).
[34] P. B. Petersen and R. J. Saykally, J. Phys. Chem. B **110**, 14060 (2006).
[35] R. Leberman and A. K. Soper, Nature (London) **378**, 364 (1995).
[36] J. D. Smith, R. J. Saykally, and P. L. Geissler, J. Am. Chem. Soc. **129**, 13847 (2007).
[37] Y. Marcus, Pure Appl. Chem. **82**, 1889 (2010).
[38] H. J. Bakker, Chem. Rev. **108**, 1456 (2008).
[39] A. S. Thomas and A. H. Elcock, J. Am. Chem. Soc. **129**, 14887 (2007).
[40] K. A. Dill, T. M. Truskett, V. Vlachy, and B. Hribar-Lee, Annu. Rev. Biophys. Biomol. Struct. **34**, 173 (2005).
[41] H. Shinto, S. Morisada, and K. Higashitani, J. Chem. Eng. Jpn. **38**, 465 (2005).
[42] Y. Ding, A. A. Hassanali, and M. Parrinello, Proc. Natl. Acad. Sci. USA **111**, 3310 (2014).
[43] J. R. Errington and P. G. Debenedetti, Nature (London) **409**, 318 (2001).
[44] P. Kumar, S. V. Buldyrev, and E. H. Stanley, Proc. Natl. Acad. Sci. USA **106**, 22130 (2009).
[45] C. Allolio, N. Salas-Illanes, Y. S. Desmukh, M. R. Hansen, and D. Sebastiani, J. Phys. Chem. B **117**, 9939 (2013).
[46] D. Laage and J. T. Hynes, Science **311**, 832 (2006).
[47] D. Laage and J. T. Hynes, Chem. Phys. Lett. **433**, 80 (2006).
[48] D. Laage and J. T. Hynes, J. Phys. Chem. B **112**, 14230 (2008).
[49] D. Laage, G. Stirnemann, F. Sterpone, R. Rey, and J. T. Hynes, Annu. Rev. Phys. Chem. **62**, 395 (2011).
[50] A. Vila Verde, P. G. Bolhuis, and R. K. Campen, J. Phys. Chem. B **116**, 9467 (2012).